Scatter correction on its own increases image contrast in Tl-201 myocardium perfusion scintigraphy, but does it also improve diagnostic accuracy?

Blokland, K.J.A.K.; de Vos tot Nederveen Cappel, W.H.; van Eck-Smit, B.; Pauwels, E.K.J.

DOI
10.1007/BF02984983

Publication date
2003

Published in
Annals of nuclear medicine

Annals of Nuclear Medicine Vol. 17, No. 8, 725–731, 2003

Scatter correction on its own increases image contrast in Tl-201 myocardium perfusion scintigraphy, but does it also improve diagnostic accuracy?

Koos (J.)A.K. Blokland,* Wouter H. de Vos tot Nederveen Cappel,*
Berthe L.F. van Eck-Smit*,** and Ernest K.J. Pauwels*

*Leiden University Medical Centre, Department of Radiology, Division of Nuclear Medicine, Leiden, The Netherlands
**Academic Medical Centre, Department of Nuclear Medicine, Amsterdam, The Netherlands

Poor and variable spatial resolution of the gamma camera, the movement of the heart and, above all, the inclusion of scattered photons in the acquisition data contribute to the deterioration of image contrast in ^{201}Tl myocardium perfusion studies. Scatter correction algorithms may correct for the latter factor by removing (most of) the scattered photons from the acquisition data. ***Methods:*** In this study we investigated the contrast changes induced by the Triple Energy Window scatter correction method (TEW) applied to clinical ^{201}Tl myocardium perfusion studies and its influence on the reading of the images. Stress and rest studies of 30 consecutive patients were used for this study. Maximum image contrasts were measured between the myocardium and the left ventricular cavity in four mid-ventricular short axis slices, as well as between normally and abnormally perfused myocardium using bull's-eye displays of the activity within the myocardium. To assess image quality and perfusion abnormalities, an experienced nuclear medicine physician, blind to patient characteristics, visually reviewed all studies. ***Results:*** In all individual measurements, the maximum contrast after scatter correction was higher than without correction ($p < 0.001$). The average increase in contrast between the myocardium and the left ventricular cavity was 43% and 48% for stress and rest studies respectively. The contrast within the myocardium increased by 25% and 32% respectively. After TEW, image quality was rated lower in almost half of the studies, while in only one study the quality was rated higher. In stress studies 11 additional perfusion defects were observed, with rest studies revealing 15 more defects after TEW, but this difference was not significant. Cohen's kappa indicated a moderate agreement of the image reading between studies with and without scatter correction. ***Conclusion:*** We conclude that image contrast improves significantly by scatter correction. However, image quality decreased as a result of an unfavorable signal-to-noise ratio. As an overall result, no significant change in the clinical outcome of the studies could be shown. Additional training of the readers may be required to obtain optimal results.

Key words: scatter correction, image contrast, myocardium perfusion study

INTRODUCTION

Visual reading of ^{201}Tl myocardium perfusion images is hampered by low image contrast resulting from poor and distant dependent spatial resolution of the gamma camera, movement of the heart and, above all, inclusion of scattered photons. These scattered photons may originate from the 135 keV and 167 keV photo peaks of thallium-201, but may also derive from other radionuclides, such as ^{99m}Tc when for instance a dual isotope protocol is used for data acquisition.[1–3] Low contrast will mask (small) defects with only a mildly reduced perfusion. It also hampers the outlining of the myocardium for further processing. Scatter correction methods may reduce this image distortion by removing (most of) the scattered

Received April 14, 2003, revision accepted September 26, 2003.

For reprint contact: Dr. ir. J. A. K. Blokland, Leiden University Medical Centre, Nuclear Medicine, C4Q-76, P. O. Box 9600, 2300 RC Leiden, The Netherlands.
E-mail: j.a.k.blokland@lumc.nl

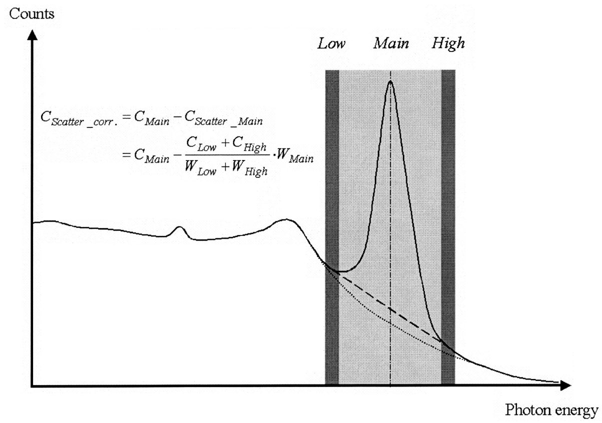

Fig. 1 Window settings in Triple Energy Window scatter correction. The main window is centered on the peak in the photon energy spectrum of the isotope; the windows used to estimate the scatter contribution are placed adjoined to the main window.

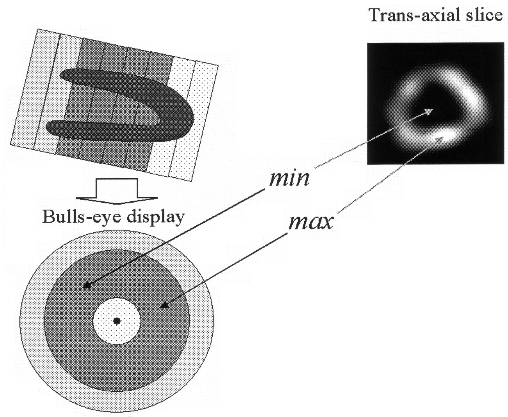

Fig. 2 Region of interest selection. Four mid-ventricular short axis slices were selected for contrast assessment, with apical and basal slices excluded. On the bull's-eye display a corresponding, band-shaped region was selected to determine the minimum and maximum count densities.

Table 1 Patient data

Patients	30 (19 male, 11 female)
Mean age (range)	60 yr (39–81 yr)
Myocardial infarction	11 (10 male, 1 female)
Stress modality	ergometric test: 25
	pharmacological test: 5

photons and thus will result in a higher image contrast.

Several methods for scatter correction have been proposed during the past years.[4–18] The triple energy window scatter correction method (TEW) presented by Ogawa et al.[15] has been shown to perform as one of the best.[19,20] TEW estimates the contribution of scattered photons to the acquisition data by means of two additional narrow energy windows (scatter windows, SWs) placed adjoined to the main energy window (MW) (Fig. 1). The scatter contribution to the MW data is estimated through a linear interpolation and, after filtering to remove some of the noise, subtracted from it.

In this study, we assessed the single influence of TEW scatter correction on contrast and image interpretation of clinical myocardium perfusion studies. Contrast was assessed between the myocardium and the left ventricular cavity. Moreover, defect severity was assessed. As the subtraction process, which is part of TEW scatter correction, may degrade the signal-to-noise ratio (SNR), we also assessed changes in interpretation of images and the appreciation of the quality of the scintigrams by the reader.

MATERIAL AND METHODS

Data acquisition

Stress and rest myocardium perfusion studies of 30 consecutive patients were used for this investigation. All patients were admitted for the evaluation of undiagnosed chest pain. Patients underwent either ergometric stress or received pharmacological stress test using dipyridamole (Table 1). At maximum stress, 75 MBq ^{201}Tl was injected followed by a re-injection of 37 MBq ^{201}Tl at rest.[21] Immediately after stress and 60 minutes after re-injection of the radiopharmaceutical SPECT projection data were acquired using a three head rotating gamma camera (GCA 9300/hg, Toshiba, Tokyo, Japan) equipped with low-energy high-resolution collimators.

A 20% main energy window was centred on the main photo peak (~70 keV) in the energy spectrum of thallium-201. Two 7% wide energy windows, used to collect information on the contribution of scattered photons to the MW data, were placed adjoining the main energy window. Projection data were acquired over 360° with the step-and-shoot method (3 × 30 projections, 4° steps) without zoom in a 128^2 matrix (3.125 mm/pixel).

Data processing

Prior to SPECT reconstruction, the MW data and the SW data were filtered separately by an order-8 Butterworth filter with cut-off frequencies equal to 0.12 cycles per pixel and 0.07 cycles per pixel respectively. During tomographic reconstruction only a Ramp filter was applied.

After reorientation of the data 8 short axis slices of almost 1 cm thickness each were obtained with the left ventricle (LV) centered in it (Fig. 2). To facilitate evaluation of myocardial perfusion, bull's-eye displays were also generated.

Contrast analysis

Contrast between the myocardium and LV cavity as well as contrast between normally and abnormally perfused myocardium was quantitatively assessed. Apical and basal regions were excluded, resulting in the analysis of only the four mid-ventricular slices. A comparable region on the bull's-eye display was selected (Fig. 2). Contrast values were determined in each of the four short axis slices separately.

Contrast was defined as

$$C = \frac{max - min}{max + min},$$

where *max* is the maximum count density found in the myocardium, either in each of the short axis slices or in the bull's-eye display, and *min* is the minimum count density found either in the LV cavity of the same short axis slice or in an area with reduced perfusion in the bull's-eye display. Contrast values were computed for each of the four analyzed short axis slices separately and for the bull's-eye display.

Defect size assessment

The size of exercise induced perfusion defects was assessed from the bull's-eye displays. According to the model of Maddahi,[22] we allocated on the bull's-eye display non-overlapping perfusion areas to the three main coronary arteries: LAD, LCx and RCA. A significant redistribution of the radiopharmaceutical on the rest image was defined as an increase of the relative count density of at least 10% of the maximum. For each of the three areas the size and the mean change of count density were determined with and without TEW.

Image reading

All studies were analyzed by an experienced nuclear medicine physician. To blind the reader to patient information and reconstruction differences, all studies were coded and randomly presented in six daily sessions of 10 patient studies each.

Data were visually assessed from the computer screen, which was showing the short axis slices and the horizontal and vertical long axis slices, as well as the bull's-eye displays. Stress and the re-injection studies were shown simultaneously. Myocardial perfusion was assessed in nine segments: ANT, AL, LAT, IL, INF, IS, SEP, AS, and Apex. A four-point scale was used, ranging from absolutely abnormal (0), via probably abnormal (1) and probably normal (2) to absolutely normal (3). Changes in the visual grading between stress and rest images were confirmed in the bull's-eye displays. In addition, the quality of each rest and stress study was graded as poor, moderate, acceptable or good (0–3).

After completion of the reading sessions the results of the scatter-corrected data were compared to those obtained with non-corrected data. An additional defect was present when the segment score changed from *absolutely normal* without scatter correction to *probably* or *absolutely abnormal* after TEW.

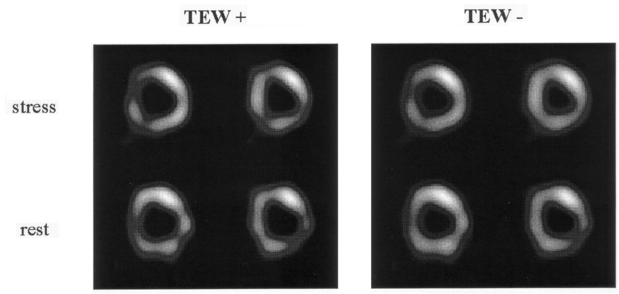

Fig. 3 Myocardial perfusion in two short axis slices of a single patient. The images show the perfusion at stress and after rest with and without scatter correction. Small perfusion defects are better visualized after scatter correction.

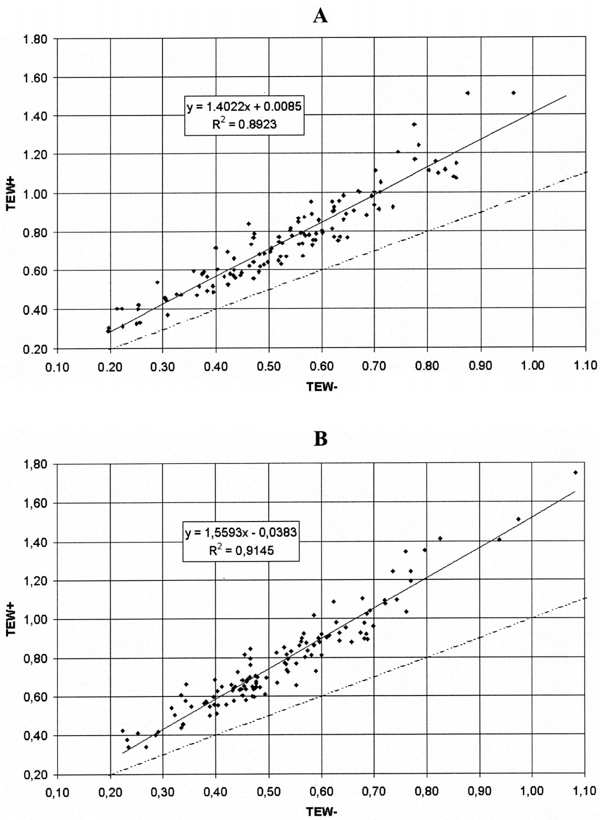

Fig. 4 Myocardium-LV cavity contrasts in stress (A) and rest (B) studies with and without scatter correction. Each point reflects the contrast in one slice of a single stress or rest study. The straight line is a linear fit through all the points. Note that all points lie above the line of identity (*dashed line*).

Statistical analysis

To assess the significance of the change in contrast, the paired-samples two-tailed t-test was used. The measurements of the contrast between the myocardium and the LV-cavity in each of the four slices of each patient study were assumed to be independent.

The agreement between scatter corrected and non-corrected studies was assessed through Cohen's kappa (Ck).

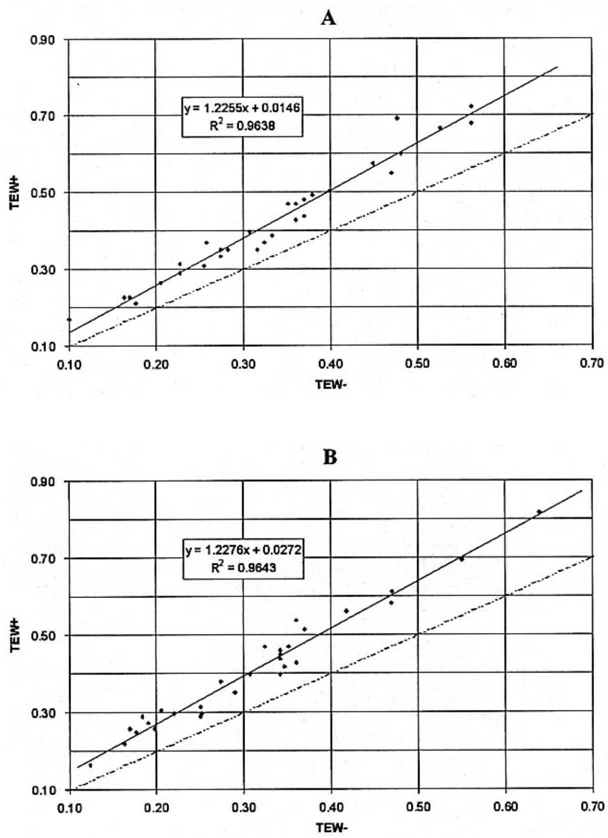

Fig. 5 Maximum contrasts between normally and abnormally perfused myocardium in stress (A) and rest (B) studies. Each point reflects the contrast assessed from the bull's-eye display of a single study.

RESULTS

Contrast improvement

Figure 3 shows a typical example of two short axis slices of a patient, with and without scatter correction. The contrast improvement can be assessed visually.

Figures 4 and 5 show the contrast changes induced by TEW scatter correction. All the points of the graphs lie above the line of identity, which means that the contrast increased in all slices of all studies, as well as in the bull's-eye displays. In the stress studies, the mean contrast between the LV cavity and the myocardium without scatter correction was 0.54 (range 0.20–0.96). After scatter correction this contrast increased significantly to 0.76 (0.29–1.51). In the rest studies, contrast improved from 0.52 (0.32–1.08) to 0.78 (0.34–1.75). The average increase of contrast was 43% for stress studies and 48% for rest studies.

The mean contrast between normally and abnormally perfused myocardium as assessed from the bull's-eye displays, increased from 0.33 (0.10–0.56) to 0.42 (0.17–0.72) for stress studies and from 0.31 (0.12–0.64) to 0.41 (0.16–0.82) for rest studies. The average increase of the contrast was equal to 25% and 32% for stress and rest studies, respectively. All contrast changes were significant at a level $p < 0.001$.

Table 2 summarizes the influence of TEW on the degree of reversibility of exercise induced perfusion defects. In most patients the defects increased in size and severity after TEW. This was also the case for defects in the LAD and LCx perfusion areas separately. The part of the left ventricular myocardium that was allocated to the

Table 2 Changes in vascular area and severity of resolving perfusion defects induced by TEW

artery	area		severity	
	increase	decrease	increase	decrease
LAD	17	7	23	4
RCA	10	16	12	15
LCx	11	11	18	7
All arteries	20	8	20	8

Table 3 Comparison of the quality scores with (+) and without (–) TEW

		TEW–				Total
		0	1	2	3	
TEW+	0	1	4	0	0	5
	1	0	1	3	4	8
	2	0	1	2	2	5
	3	0	0	0	11	11
Total		1	6	5	17	29

Table 4 Comparison of segmental scores in stress studies with (+) and without (–) TEW. The additional defects found after scatter correction are shown in italics

		TEW–				Total
		0	1	2	3	
TEW+	0	70	11	5	*3*	89
	1	1	5	9	*8*	23
	2	0	2	10	20	32
	3	1	1	7	108	117
Total		72	19	31	139	261

Table 5 Comparison of segmental scores in rest studies with and without TEW. The additional defects found after scatter correction are shown in italics

		TEW–				Total
		0	1	2	3	
TEW+	0	41	13	6	*6*	66
	1	0	1	6	*9*	16
	2	1	0	11	38	50
	3	0	1	2	126	129
Total		42	15	25	179	261

RCA artery showed the opposite behavior: after TEW the defects were in general, smaller and less severe.

Image reading

In one TEW corrected patient study, visual analysis was considered impossible due to poor quality. Without correction, the quality of this study was judged as moderate. This study is not included in the following results.

Despite the increased image contrast in all studies, image quality was rated lower in 13 studies and did not change in 15. Quality was improved in only one study. Before scatter correction, the image quality of 22 of 29 studies was rated as good or acceptable (Table 3). After TEW, 15 of 22 studies were still rated as good or acceptable, and quality worsened in 9 studies, but was never downgraded to poor.

Tables 4 and 5 summarize the segmental stress and rest scores before and after TEW. The mean segmental score decreased from 1.91 to 1.68 and from 2.31 to 1.93 for exercise and rest studies respectively. The segmental perfusion score changed through TEW: for exercise studies, 56 segments received a lower score and 12 were judged to have a better perfusion. In rest studies the number of changes was even larger, 78 segments were rated lower and in only 4 segments an improved perfusion was decided to be present. The TEW procedure yielded 11 additional defects (1×3; 1×2) in 8 stress studies. In rest studies, 15 additional defects were scored in 12 studies that were judged as normal without TEW. Small, non-significant changes were observed in 20 myocardial segments of stress studies and in 38 segments of rest studies. A moderate agreement between the rating before and after TEW was found: Cohen's kappa was equal to 0.60 and 0.48 for exercise and rest studies, respectively. The maximum relative perfusion change between stress and rest studies, as obtained from the bull's-eye displays increased after applying TEW in 28 of 29 patient studies. In 3 patient studies this difference changed from a value below to above the threshold of 10%.

DISCUSSION

In this study, we have shown considerable image contrast improvements by only applying TEW in clinical ^{201}Tl perfusion studies. In all slices of all studies, as well as in the corresponding bull's-eye displays contrast increased. This increased contrast may facilitate the reading of the patient studies. But, at the same time, the scatter correction process, subtracting two noisy signals, will lead to a reduced signal and an increased noise. The final result will be a reduction of the SNR, with noise being the major degrading factor. The worsening of the SNR may nullify the improved readability of the images. Therefore, to keep the SNR at a reasonable level, we applied low pass filters to the MW data as well as to the estimate of the scatter contribution. In a previous phantom study, we have optimized the filter parameters to obtain maximum SNR values.[23] We used these optimized parameter values in the present study. Nevertheless, after scatter correction, we still obtained sometimes poor images, but only in those studies that already had a (visually) low initial SNR and were qualified as poor. Only one study rendered unreadable through TEW.

A few minutes after injection, the amount of circulating ^{201}Tl will be negligible. So, for the contrast between the myocardium and the LV cavity after scatter correction, one may expect values close to 1.00. In a few studies we have found very high contrasts (>1.00). Negative pixel values resulting from reconstruction filter over and under shoots explain these high contrasts, even before scatter correction. Negative numbers are not set to zero in our Toshiba computer system, but will be displayed as pixels with zero values. Overcompensation of the scatter may cause additional (too) high values. Contrast values much smaller than 1.00 even after TEW may be also due to partial volume effects and the motion of the ventricle during acquisition. ECG gating during acquisition was not applied in this study. Also, attenuation will affact the contrast values. This influence, however, will be the same for studies processed with and without scatter correction.

Another cause for overcompensation of the scatter component in the main energy window may be found in the window settings. In daily clinical practice, we center the 20% main energy window on the peak (~70 keV) in the photon energy spectrum. By doing so, not only some "good" ^{201}Tl photons with energies around 80 keV are excluded, but also characteristic lead X-rays. These X-rays (in the 80–90 keV range) are caused by interactions of the high energy photons (135 keV and 167 keV) of ^{201}Tl with the collimator. These X-rays do not contain the direction information of the interacting photons and should not be included in the image. To be able to compare scatter corrected with non-corrected data using a single acquisition, the main window setting was not changed in this study. Therefore, the upper scatter window that is positioned adjoined to the main window may contain too many counts, resulting in an overestimation of the scatter contribution to the main window.

In this study, we only assessed the contrast defined as the maximum differences in count densities. This type of measurement may be noise sensitive. However, the filtering of the data removes much of the noise. In fact, the data are not obtained from a single pixel, as it combines information from many neighboring pixels. Due to the noise, the increase of contrast between myocardium and LV cavity, ranging from 43% to 48%, may be a bit overestimated. When creating the bull's-eye displays an additional smoothing is involved, resulting in a lower increase of contrast between defects and normally perfused myocardium.

Because the scatter fraction is spatially variant, the correction will be different from point to point. So, the maximum contrast may be found at different locations before and after scatter correction. We did not assess the location of the minimum and maximum values. The change in maximum contrast does not necessarily reflect the local changes, which may be different.

We measured the image contrast in two ways, between the LV cavity and myocardium as well as between normally and abnormally perfused myocardium. Optimal contrast between the myocardium and its cavity will facilitate the delineation of the myocardium. Increased contrast within the myocardium will make perfusion defects easier to assess. One can also use dedicated color scales aimed to visualize small differences in count densities. This method, however, does not correct for the errors (inclusion of the scattered photons), but only makes small differences easier to assess.

Another way to increase visual image contrast is the subjective change of the brightness and contrast settings either of the monitor used to display the image, or by software. Such a contrast adaptation, however, will introduce a global change of the image and is difficult to reproduce. TEW will change the contrast locally by correcting point by point for the estimated local scatter contribution.

To our knowledge, no other study focussing solely on contrast changes in clinical myocardium perfusion studies has been published up to now. Yang et al. studied count ratios in dual isotope myocardial studies using ^{123}I-labeled fatty acid (BMIPP) and ^{201}Tl.[24] To measure the count densities they used profiles through a perfusion defect and the center of the LV-cavity. Thus, they compared defect counts with the count density in the opposite myocardium, which was assumed to be normally perfused. In a Monte Carlo and phantom study, El Fakhri et al. analyzed methods to correct for several image degrading factors including scatter.[25] They also found that scatter correction significantly improved contrast, but reduced SNR. In two other studies, contrast and signal-to-noise ratios were analyzed for brain and liver images respectively. Gustafsson et al. found comparable results in a Monte Carlo brain study: "... contrast was improved, but the contrast(signal)-to-noise ratio was made worse."[26] In a phantom study, Perisinakis et al. found a mean contrast increase of 1.7 but at the cost of a degradation of the SNR.[27] This increase of contrast is comparable with the increase noted in our study.

In the present study, we measured contrast changes induced by TEW. Although contrast values significantly improved in all studies we could not show a significantly different clinical outcome. Cohen's kappa, reflecting the similarity of the results before and after TEW, was around 0.5 for rest as well as for stress. Thus, there was a moderate agreement between scatter corrected and non-corrected studies.

Image reading was performed in a similar way for scatter corrected and non-corrected images, the readers were not trained to judge the scatter corrected studies. To discriminate between real and artificial defects, the same mental thresholds were applied to scatter corrected and non-corrected data. Afterwards reading results were compared to the available clinical data of the patients. The additional defects found after scatter correction were significant in size and severity and were not in conflict with the clinical status of the patients. Obviously, no golden standard was available for this clinical study. Different (visual) thresholds to distinguish perfusion defects from normally perfused myocardium may have to be applied for corrected and non-corrected data. Training of the operators, however, would have required a considerable number of studies with well-defined abnormalities. Such a study was not considered relevant within the scope of our investigations. However, it will be required when changing any imaging protocol in clinical use.

Overall we have found more and more severe defects after scatter correction. The perfusion territories of the RCA (inferior), however, showed the opposite behavior compared to the myocardial segments perfused by the LCx and LAD arteries (anterior and antero-septal). The differences in depth of these myocardial segments in the patient body will result in different attenuation of particularly the scattered lower energetic photons and so in the relative contribution of scattered photons.

In this single isotope study the scattered photons originate mainly from the higher energy photons emitted by ^{201}Tl. In dual-isotope studies, to image stress and rest perfusion in one acquisition, the amount of scatter may be more prominent. Retraining of the operator to deal with these images, whether they are scatter corrected or not, will be required.

CONCLUSIONS

Triple Energy Window scatter correction significantly improves the contrast between the LV myocardium and the LV cavity, as well as between normally perfused myocardium and regions with reduced perfusion. This improved contrast makes the images easier to read and should result in an improved clinical outcome of an individual patient study. However, improved accuracy could not be observed in the present study with a limited number of patients, which may be due to a decreased signal-to-noise ratio.

REFERENCES

1. Kiat H, Germano G, Friedman J, Van Train K, Silagan G, Wang FP, et al. Comparative feasibility of separate or simultaneous rest thallium-201/stress technetium-99m-sestamibi dual-isotope myocardial perfusion SPECT. *J Nucl Med* 1994; 35: 542–548.
2. Lowe VJ, Greer KL, Hanson MW, Jaszczak RJ, Coleman RE. Cardiac phantom evaluation of simultaneously acquired dual-isotope rest thallium-201/stress technetium-

99m SPECT images [see comments]. *J Nucl Med* 1993; 34: 1998–2006.

3. Ando H, Fukuyama T, Mitsuoka W, Egashira S, Imamura Y, Masaki H, et al. Influence of downscatter in simultaneously acquired thallium-201/technetium-99m-PYP SPECT. *J Nucl Med* 1996; 37: 781–785.
4. Axelsson B, Msaki P, Israelsson A. Subtraction of Compton-scattered photons in single-photon emission computerized tomography. *J Nucl Med* 1984; 25: 490–494.
5. Msaki P, Axelsson B, Dahl CM, Larsson SA. Generalized scatter correction method in SPECT using point scatter distribution functions. *J Nucl Med* 1987; 28: 1861–1869.
6. Naimuddin S, Hasegawa B, Mistretta CA. Scatter-glare correction using a convolution algorithm with variable weighting. *Med Phys* 1987; 14: 330–334.
7. Singh M, Horne C. Use of a germanium detector to optimize scatter correction in SPECT. *J Nucl Med* 1987; 28: 1853–1860.
8. Halama JR, Henkin RE, Friend LE. Gamma camera radionuclide images: improved contrast with energy-weighted acquisition. *Radiology* 1988; 169: 533–538.
9. Mukai T, Links JM, Douglass KH, Wagner HN Jr. Scatter correction in SPECT using non-uniform attenuation data. *Phys Med Biol* 1988; 33: 1129–1140.
10. Fleming JS. A technique for using CT images in attenuation correction and quantification in SPECT. *Nucl Med Commun* 1989; 10: 83–97.
11. Wagner FC, Macovski A, Nishimura DG. Two interpolating filters for scatter estimation. *Med Phys* 1989; 16: 747–757.
12. Mas J, Hannequin P, Ben Younes R, Bellaton B, Bidet R. Scatter correction in planar imaging and SPECT by constrained factor analysis of dynamic structures (FADS). *Phys Med Biol* 1990; 35: 1451–1465.
13. Koral KF, Swailem FM, Buchbinder S, Clinthorne NH, Rogers WL, Tsui BM. SPECT dual-energy-window Compton correction: scatter multiplier required for quantification. *J Nucl Med* 1990; 31: 90–98.
14. King MA, Hademenos GJ, Glick SJ. A dual-photopeak window method for scatter correction. *J Nucl Med* 1992; 33: 605–612.
15. Ogawa K. Simulation study of triple-energy-window scatter correction in combined Tl-201, Tc-99m SPECT. *Ann Nucl Med* 1994; 8: 277–281.
16. Pretorius PH, van Rensburg AJ, van Aswegen A, Lotter MG, Serfontein DE, Herbst CP. The channel ratio method of scatter correction for radionuclide image quantitation. *J Nucl Med* 1993; 34: 330–335.
17. Meikle SR, Hutton BF, Bailey DL. A transmission-dependent method for scatter correction in SPECT. *J Nucl Med* 1994; 35: 360–367.
18. Chen EQ, Lam CF. Predictor-corrector with cubic spline method for spectrum estimation in Compton scatter correction of SPECT. *Comput Biol Med* 1994; 24: 229–242.
19. Buvat I, Rodriguez Villafuerte M, Todd Pokropek A, Benali H, Di Paola R. Comparative assessment of nine scatter correction methods based on spectral analysis using Monte Carlo simulations. *J Nucl Med* 1995; 36: 1476–1488.
20. Ljungberg M, King MA, Hademenos GJ, Strand SE. Comparison of four scatter correction methods using Monte Carlo simulated source distributions. *J Nucl Med* 1994; 35: 143–151.
21. van Eck Smit BL, van der Wall EE, Zwinderman AH, Pauwels EK. Clinical value of immediate thallium-201 reinjection imaging for the detection of ischaemic heart disease. *Eur Heart J* 1995; 16: 410–420.
22. Maddahi J, Van-Train K, Prigent F, Garcia EV, Friedman J, Ostrzega E, et al. Quantitative single photon emission computed thallium-201 tomography for detection and localization of coronary artery disease: optimization and prospective validation of a new technique. *J Am Coll Cardiol* 1989; 14: 1689–1699.
23. Blokland KAK, Winn RDR, Pauwels EKJ. Signal to noise ratio based filter optimization in triple energy window scatter correction. *Medical Physics* 2000; 27: 1955–1960.
24. Yang JT, Yamamoto K, Sadato N, Tsuchida T, Takahashi N, Hayashi N, et al. Clinical value of triple-energy window scatter correction in simultaneous dual-isotope single-photon emission tomography with ^{123}I-BMIPP and ^{201}Tl. *Eur J Nucl Med* 1997; 24: 1099–1106.
25. El Fakhri G, Buvat I, Benali H, Todd Pokropek A, Di Paola R. Relative impact of scatter, collimator response, attenuation, and finite spatial resolution corrections in cardiac SPECT. *J Nucl Med* 2000; 41: 1400–1408.
26. Gustafsson A, Arlig A, Jacobsson L, Ljungberg M, Wikkelso C. Dual-window scatter correction and energy window setting in cerebral blood flow SPECT: a Monte Carlo study. *Physics In Medicine And Biology* 2000; 45: 3431–3440.
27. Perisinakis K, Karkavitsas N, Damilakis J, Gourtsoyiannis N. Effect of dual and triple energy window scatter correction methods on image quality in liver scintigraphy. *Nuklearmedizin* 1998; 37: 239–244.